Amirkabir University of Technology
(Tehran Polytechnic)
Vol. 46, No. 2, Fall 2014, pp. 47- 55

Amirkabir International Journal of Science& Research
(Electrical & Electronics Engineering)
(AIJ-EEE)

Decentralized Frequency Restoration in Islanded Converter Base Microgrid

M. Kosari[1], S. H. Hosseinian[2*] and A. Mahmoudi[1]

1-PhD. Student, Department of Electrical Engineering, Amirkabir University of Technology, Tehran, Iran
2-Professor, Department of Electrical Engineering, Amirkabir University of Technology, Tehran, Iran

ABSTRACT

Variation of frequency and voltage by load changes in a microgrid is a challenge in droop control method. Centralized restoration frequency or voltage in a microgrid requires communication link and therefore affects the advantage of decentralized droop control such as reliability, simplicity and inexpensiveness. This paper proposes a decentralized method that restores the frequency of a microgrid without any communication link and maintains these advantages. The method detects signal changing by wavelet transform (WT) to synchronize distributed energy resource (DER) that interfaced by converter to microgrid. Its operation principle and control method are explained and analyzed. The simulation results are presented to validate the effectiveness of the proposed method.

KEYWORD

Decentralized Frequency restoration, Droop control, Wavelet transform.

* Corresponding Author, Email: hosseinian@aut.ac.ir

1- INTRODUCTION

Microgrid is a solution and an effective mean of integrating various DERs such as photovoltaic, fuel cells, wind turbines, microturbines, etc., to provide electric power of high quality and reliability through their interface converters. Microgrids can be used to operate in two modes: grid connected and islanded mode. In grid connected mode, most of the system dynamics are dictated by the main grid due to the relatively small size of DERs. In this mode, DERs usually generate constant active power. In an islanded mode, the microgrid is responsible for system dynamic and conventionally, the DER interface converters (DIC) of the microgrid are governed by droop control algorithms for the autonomous power sharing operations between DERs and maintaining the voltage regulation and frequency regulation in the microgrid [1-7].

However, the droop method as the decentralized control strategies can operate in an autonomous fashion without any communication link, and therefore increases reliability and simplicity but it encounters with some challenges. The first challenge is the deterioration in reactive power sharing among DIC units due to its dependence on the line impedances. Previous work done in [7-11] proposes some efforts for solving this drawback.

Variation of frequency and voltage by load changing in the microgrid is another challenge of droop method [12-14]. In these papers, restoration of frequency and voltage is presented as the secondary control level in a hierarchical control of the microgrid. In these methods, the control of the microgrid is supposed to be centralized and the frequency and voltage deviation from the nominal value is determined in the central control and then transmitted to DICs in the microgrid to restore them. Therefore, the communication link is needed and the advantages of decentralize control such as reliability, simplicity and inexpensiveness are affected.

This paper presents a decentralized method for frequency restoration that does not need any communication link between DERs and therefore retains the advantages of decentralize control. The proposed method used load change point for synchronizing DICs in the microgrid.

The remainder of this paper is organized as follows. Section II begins by introducing the existing power–frequency (P−f) and reactive power–voltage (Q−V) droop control. Section III explains the proposed restoration method. Signal change detection by wavelet is presented in section IV. Finally, the simulation result and conclusion are given in section V and VI , respectively.

2- FREQUENCY AND VOLTAGE DROOP CONTROL

Droop method is based on the proportionality of real power flow to phase angle difference and reactive power flow to voltage magnitude difference between two nodes separated by a dominant inductive branch. Therefore, the control of the active power from each DIC unit can be done by varying the DIC output frequency that makes changes the phase angle dynamically. The DIC reactive power can

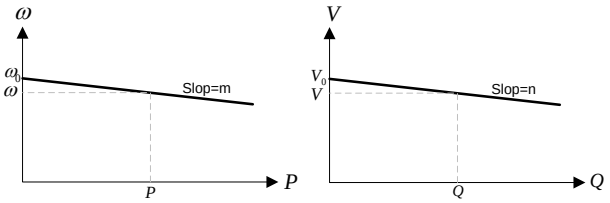

Fig. 1. P-w and Q-V droop curve

be controlled and regulated by changing the DIC output voltage magnitude [1-7]. The equation of the P-f droop characteristic is given as:

$$\omega_i = \omega_0 - m_i P_i \quad (1)$$

where i is the index number of DIC units, ω_i is the operating frequency set point of ith DIC units, ω_0 is the nominal system frequency of the microgrid (typically 50 or 60Hz), m_i is the slop of droop characteristic curve andP_i is the actual loading of the ith DIC unit. If the slopes are chosen such that:

$$m_1 P_{1r} = m_2 P_{2r} = \cdots = m_N P_{Nr} \quad (2)$$

where N is the number of DIC units and P_{ir} is the rating of ith DIC unit, then the DIC units share the total load in the microgrid in proportion to their power ratings[2]. This power sharing is independent of the number of DIC unit connected to the microgrid and does not need any data communication to control their power dispatch. In a similar manner, the equations of the$Q-V$ droop characteristic for tuning the magnitude set point of each DIC output voltage to control the flow of reactive power within the microgrid are given as:

$$V_i = V_0 - n_i Q_i \quad (3)$$

where V_i is the magnitude of output voltage, V_0 is the nominal system voltage, $n_i$is the slop of droop curve andQ_i is the actual reactive power of the ith DIC unit in the microgrid. Typically, $P-\omega$ and $Q-V$ droop curves are shown in Fig. 1.

The typical DIC control block diagram is shown in Fig. 2. The output voltage and current are fed back and transformed into the synchronous reference frame. The output real power and reactive power are calculated and then filtered by a low-pass filter [16].

The resulting P and Q are applied to the droop controller to produce the frequency $\omega$and the voltage magnitude V. Then, the voltage reference of converter $v_o^*$is synthesized in the synchronous reference frame by $\omega$and V. The voltage reference v_o^* is then applied to voltage controller and current controller, to produce the pulsewidth modulation commands of the converter [16].

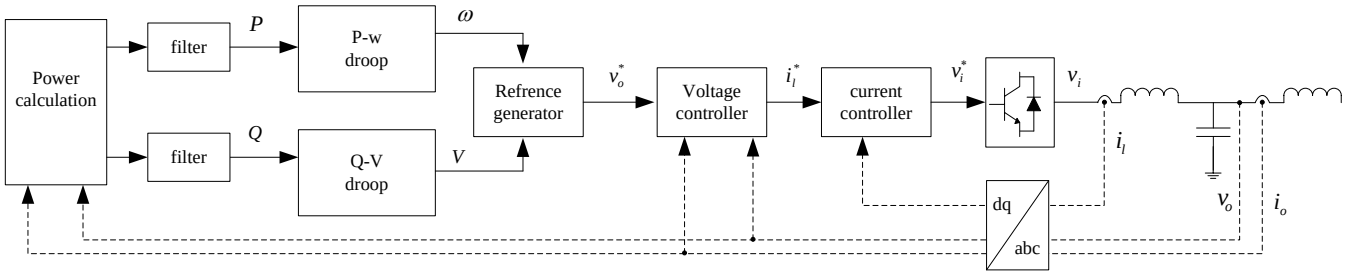

Fig. 2. The DIC unit control block diagram

3- DECENTRALIZED FREQUENCY RESTORATION

Equation (1) implies that the overall system frequency will change with changing the loads. If the slopes m_i of N DIC units connected to the microgrid are chosen by (2), then for a total load change ΔP_l, the power sharing and the steady-state frequency deviation from the nominal frequency ω_0 are [2]:

$$\Delta P_i = \frac{\Delta P_l}{m_i \sum_{j=1}^{N} \frac{1}{m_j}} \tag{4}$$

$$\Delta\omega = \frac{\Delta P_l}{\sum_{j=1}^{N} \frac{1}{m_j}} \tag{5}$$

Fig. 3 shows this situation for the two-DIC in which for simplicity, the droop curves are shown back to back. In this figure, the condition is shown by points a and a' before a load change, with nominal operating frequency ω_0. After the change in load, from P_{L1} to P_{L2}, the operating points shift to b and b', which have a lower operating frequency. To have a steady-state operating frequency, which is independent of load and at the same time ensures the correct real power sharing, the droop characteristics have to be shifted up equally between DIC units to pass through points d and d'. This restores the frequency to its nominal value ω_0. In (1), to perform this curve shifting, the control term $\delta\omega_i$ is added as follows:

$$\omega_i = \omega_0 + \delta\omega_i - m_i P_i \tag{6}$$

Refer to (6), for the frequency setting ω_i to be equal to the nominal frequency ω_0, the quantity $\delta\omega_i$ must be equal to $m_i P_i$. Thus, the quantity $\delta\omega_i$ is modified so that in the steady state, $\delta\omega_i = m_i P_i$. To achieve this, $\delta\omega_i$ is changed at the following rate:

$$\frac{d(\delta\omega_i)}{dt} = k\Delta\omega_i \tag{7}$$

where $\Delta\omega_i$s are locally measured frequency errors as:

$$\Delta\omega_i = \omega_0 - \omega_i \tag{8}$$

and k is a constant value and determines the overall rate of the frequency restoration. If the rates of changes of $\delta\omega_i$ are chosen as above, then the dynamics of the frequency error are determined by the following simple analysis from (1):

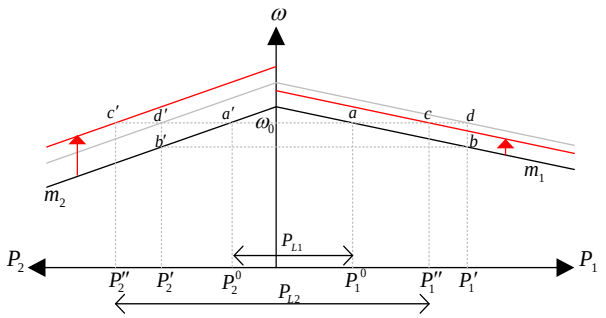

Fig. 3. Effect of not equal droop curve moving on real power sharing of two DIC units.

$$\frac{d}{dt}(\Delta\omega_i) = \frac{d(\delta\omega_i)}{dt} = k\Delta\omega_i \tag{9}$$

The solution of the equation is:

$$\Delta\omega_i(t) = \Delta\omega e^{-t/\tau_r} \tag{10}$$

$$\tau_r = -\frac{1}{k m_i P_{ir}} \tag{11}$$

Equations (10) and (11) indicate that the frequency error decays exponentially to zero, at a rate determined by the restoration time constant τ_r, which depends on the gain k. The frequency restoration method is shown schematically in the control block diagram of Fig. 4.

If the shifted up occurs unequally, the real power sharing encounters a sustained error. For example, suppose for a two DIC unit shown in Fig.3, the second DIC is moved more than the first DIC. This results in points c and c´ in the figure and variation of real power sharing between two units where unit 2 power increases from P_2' to P_2'' and unit 1 power decreases from P_1' to P_1''. Vertical moving value of each DIC unit ($\delta\omega_i$) is determined by integral of $\Delta\omega_i$ as shown in Fig.4. The $\Delta\omega_i s$ are different in DIC units, since the dynamic response of each DIC unit is different especially in the early time of load change and it makes the $\delta\omega_i$ unequal. For example, Fig. 5 shows dynamic response of two DIC units and the product of hatch area at k constant is the difference in vertical moving of the two DIC units. To decrease the effect of this inequality in the DIC units, the k constant should be decreased, but this action not only doesn't remove the error totally but also increases restoration time constant τ_r based on (11).

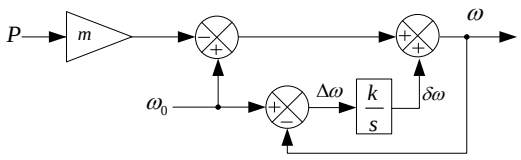

Fig. 4. Main frequency restoration method block diagram.

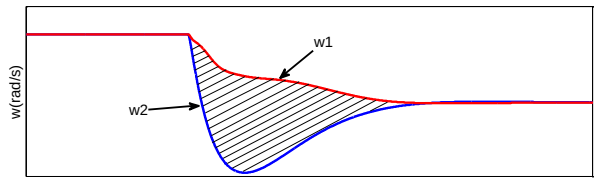

Fig. 5. Dynamic respond of two DIC units, the product of hatch area with k constant is the difference in vertical moving of two DIC units.

To remove the error of not proper sharing of restoration process, the $\delta\omega_i$ must be equal in all DIC units. For this, restoration process should be started after smoothing the dynamic response. The important problem in this solution is that the DIC units synchronizing should be carried out without any communication link. If the microgrid load is changed or other phenomena are taken place, the electrical quantity has been change suddenly. If this change is detected in each DIC units, it can be used as the synchronizing signal and the time origin. The change detection method is proposed in the next section.

After any change detection, a time duration T must be calculated to assure that all dynamics are suspended, before restorations are started. This time duration will be equal for all DIC units and can be three times of the slowest DIC units time constant which is the one with the smallest $m_i$in the migrogrid (based on the stability and root locus analysis [15-19]). If the change is also taken place in the time duration T or restoration process, the restoration is stopped and the time duration T is calculated again from this new point. This method is shown schematically in Fig. 6. Since the dynamics are suspended after the time duration T, coefficient k can be large enough to decrease the restoration time constant without making error in sharing power between DIC units.

4- CHANGE DETECTION BY WAVELET TRANSFORM

Wavelets are mathematical functions with time-frequency representation of any signal for the analysis of a signal with transient features. The wavelets are scaled and translated copies (known as "daughter wavelets") of a finite-length or fast-decaying oscillating waveform (known as the "mother wavelet"). Usually, the wavelet transform (WT), that is the representation of a function by wavelets, is expressed by a multiresolution decomposition algorithm which uses the orthogonal wavelet bases to decompose the actual signal to components under different scales with assignment of a frequency range to each scale component. Each scale component can be studied with a resolution that matches its scale.

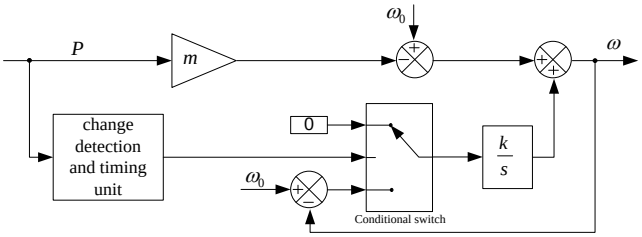

Fig. 6. Proposed frequency restoration block diagram

WT have some advantages over traditional Fourier transforms for representing functions that have discontinuities and sharp peaks that are very vital in our study. Likewise, Wavelet is better for an accurate deconstructing and reconstructing finite, non-periodic and/or non-stationary signals. The continuous WT for a given signal x(t) at a scale a and translation factor b is expressed by the following integral [20]:

$$W_{a,b}(t) = \frac{1}{\sqrt{|a|}} \int_{-\infty}^{\infty} x(t)\psi\left(\frac{t-b}{a}\right) dt \qquad (12)$$

where $\psi(t)$ is the mother wavelet. The coefficients of WT are defined by the following inner product:

$$C(a,b) = \int_0^{\infty} x(t) W'_{a,b}(t) dt \qquad (13)$$

In other words, WT can be extracted as a series of filters (bandpass), containing successive pairs of low-pass and high-pass filters that are used to show approximate and detailed coefficients. The approximations are the high-scale, low frequency components of the signal produced by filtering the signal by a low-pass filter. The details are the low-scale, high frequency components of the signal produced by filtering the signal through a high-pass filter. The detailed coefficients provide vital information for time-localizing transient events at different levels of decomposition.

Here, WT is used to detect the changing moment of signal. At each time step a window with the determined length containing current time step of signal is constructed, then decomposed by wavelet to approximate and detailed coefficients. In normal pattern of signal, coefficients of details are very low and noisy value but at the time of signal changing, they will be so large. This large difference is used for the detection of changing moment. So, the coefficients are compared with threshold and if it is bigger than the threshold, the timing process is started. It is worth to say that the coefficients are large only near the change point and then decrease rapidly.

5- SIMULATION STUDY

A microgrid model has been established using MATLAB/Simulink. As shown in Fig. 7, the simulated microgrid is composed of three DIC units with control of each DIC unit as Fig. 2. Detailed control is based on [16] which its control block parameters are given in Table 1. Power rating of DIC1 and DIC3 are 10kVA and power

TABLE 1.
DETAILED CONTROL BLOCK PARAMETERS [15]

	parameter	value
Output filter	C_f	50 µF
	L_f	1.35 mH
	r_f	0.1Ω
Output impedance	L_c	0.35 mH
	r_{Lc}	0.03Ω
Voltage controller	K_{pv}	0.05
	K_{iv}	390
	F	0.75
Current controller	K_{pc}	10.5
	K_{ic}	16e3
cut-off frequency	w_c	31.41

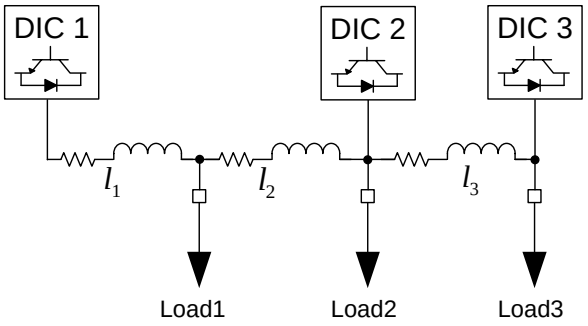

Fig. 7. Circuit configuration for computer simulations.

rating of DIC2 is 20kVA. The system parameters are given as follows:

1) The system voltage is 380V (RMS, line-to-line), ω=314 rad/s (f=50Hz);

2) Line impedances are $l_1 = 0.25 + j0.1\Omega; l_2 = 0.3 + j0.4\Omega; l_3 = 0.2 + j0.1\Omega$;

3) P-W slop drops are $m_1 = 0.5 \times 10^{-4}$; $m_2 = 0.25 \times 10^{-4}; m_3 = 0.5 \times 10^{-4}$;

4) Q-V slop drops are $n_1 = 1.2 \times 10^{-3}; n_2 = 0.6 \times 10^{-3}; n_3 = 1.2 \times 10^{-3}$;

5) Integral gain in main restoration method (Fig. 4) is k=0.3 that makes overall restoration time about 10s, a typical value.

6) Integral gain in the proposed restoration method is k=1 and duration time is T=1.5s, that make overall restoration time equal to 3s.

7) Load1=10kW+j4kVar; load2=10kW+j4kVar;unbalanced load3 ($R_{Phase,A}$=5Ω; $R_{Phase,B}$=70Ω; $R_{Phase,C}$=∞)

5-1 SUSTAINED ERROR IN REAL POWER SHARING IN MAIN RESTORATION METHOD

Suppose that at the first study, there is not any frequency restoration and load1(10kW,4kVar) is connected to the network. The frequency and power of three DIC units are depicted in Fig. 8. Finally, after the suspension transient, the frequency is 313.875 rad/s (0.125 rad/s deviation from normal), P1=P3=2500W and P2= 5000W. These values are referenced as the actual value in the next cases.

Now, main restoration method based on the block diagram in Fig.4 is applied. The frequency and power of three DIC units in this case are shown in Fig. 9. Frequency is starting to back to nominal at the same time as the load is added. By determined coefficient k=0.3, restoration time takes about 10s. Final real power of DIC units are P1= 2645W with 145W (+5.8%) deviation from actual value, P2=4894W with -151W (-2.1%) deviation from actual value and P3=2451W with -49W (-2%) deviation from actual value. These deviations from actual value are resulted from the difference in transient response of DIC units. Fig. 10 shows the frequency error and its integration that determined vertical moving value for each DIC unit characteristic.

5-2 THE PROPOSED RESTORATION METHOD

In this case study, the proposed restoration method is applied and the same load like before is added. The frequency and real power of DIC units are shown in Fig 11. As seen, after the load is added, the duration time T=1.5s is accounted and then the frequency is starting to back to the nominal value. Since the frequency error and then its integration is equal in DIC units at the moment of starting restoration process, the vertical moving value rate of DIC units are the same and there is no transient in the real power and also no deviation from the actual value (P1=P3=2500 and P2=5000 the same as actual value).

To illustrate what happened if the load is changed in the restoration process and also illustrated the performance of proposed method on unbalance load, the system is supposed to be in a steady state with load1 and this scenario is executed: load2 is added at 3s and unbalanced load3 is added and removed at 4s and 5.8s, respectively. Frequency and power of DIC units are shown in Fig. 12. At the time 3s, the first load change is taken place and timer starts to account duration time T. At time 4s where value of T is 1s, next load change is taken place and the timer is reset and duration time T is accounted from this moment again. At time 5.5s duration Time T that its account starting from last load change elapsed and frequency is starting to back to nominal. Among this situation, next load change takes place at 5.8s, so restoration is stopped and duration T is started from this new point again. So the proposed method is strong even in an unbalanced load that is a typical situation in the practical network.

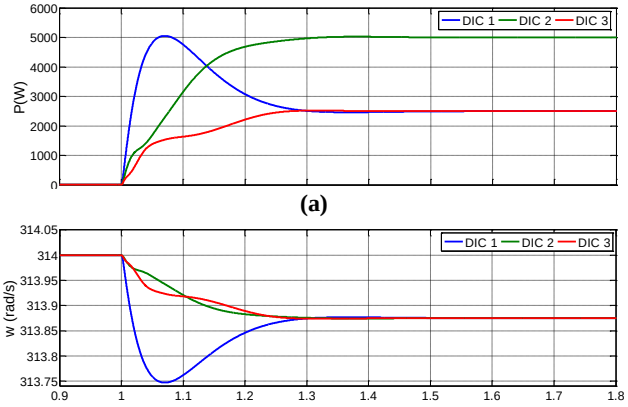

(a)

(b)

Fig. 8. The real power (a) and frequency (b) of three DIC units without any restoration (Load1 is added on 1s).

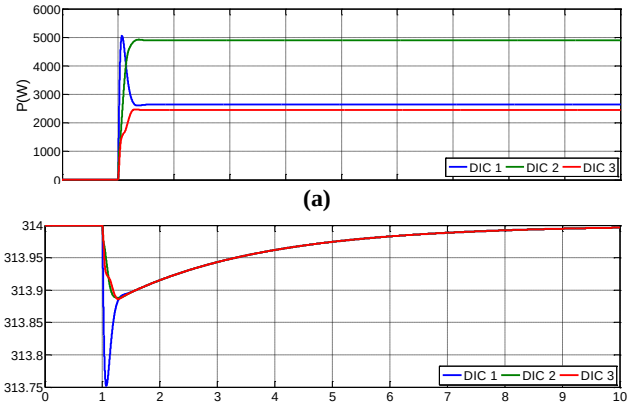

(a)

(b)

Fig. 9. The real power (a) and frequency (b) of three DIC units with main restoration method (Load1 is added on 1s).

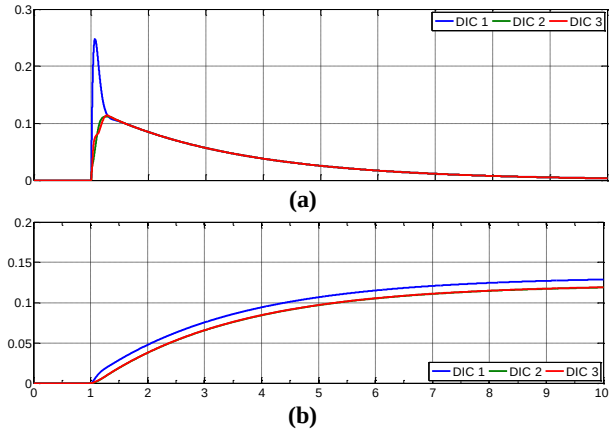

(a)

(b)

Fig. 10. Three DIC units locally measured frequency errors (a) and its integral (b). ($\Delta\omega$) ($\delta\omega$)

5-3 SYNCHRONIZING BY WAVELET TRANSFORM

Performance of WT for change detection that is the basis of the proposed restoration method is illustrated here. For this, different load change in position of load1 to load3 is accomplished to cover the small value as well as the large value load changes. Here, a window of 64 time step is analyzed by the tenth order daubechies wavelet (db10).

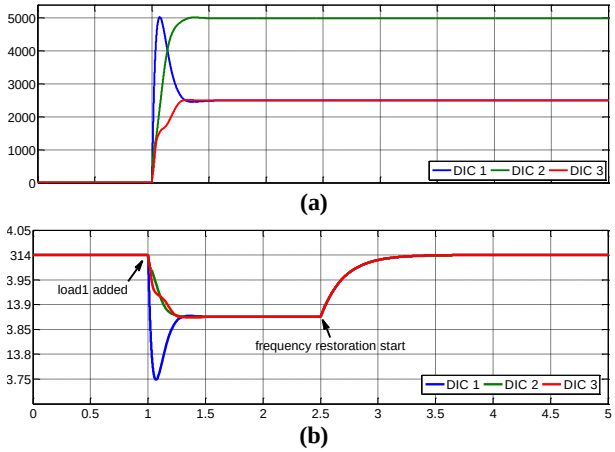

(a)

(b)

Fig. 11. The real power (a) and frequency (b) of three DIC units with proposed restoration method (Load1 is added on 1s).

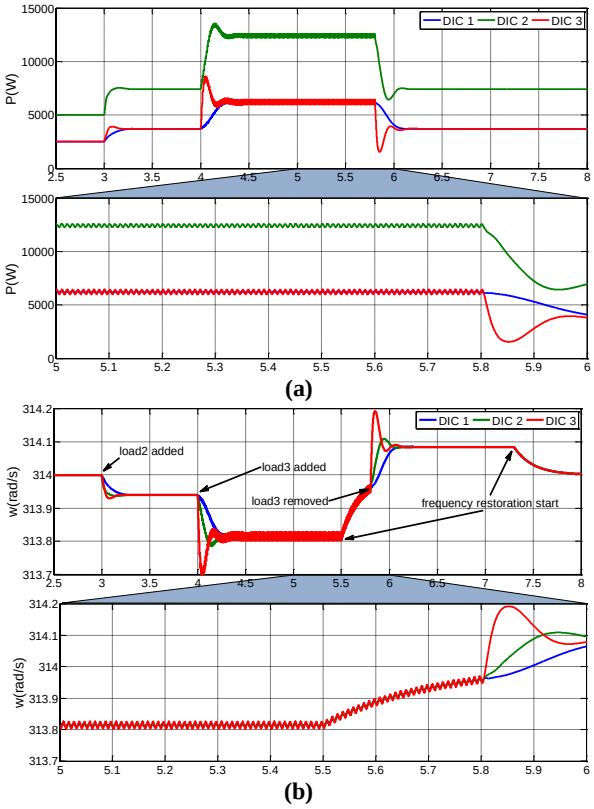

(a)

(b)

Fig. 12. The real power (a) and frequency (b) of three DIC units with proposed restoration method. load2 is added at 3s and unbalanced load3 is added and removed at 4s and 5.8s respectively.

Time, situation, absolute value of detail coefficient before and after load change and the ratio of them are summarized in Table 2. Power and absolute detail coefficient value in this case are shown in Fig. 13 and Fig. 14, respectively. As seen in the Table 2, before the load change, detail coefficients are noisy value and are under 1e-10, but after the load change, these coefficients increase significantly.

TABLE 2.

DETAIL COEFFICIENT OF DIC UNITS WITH VARIOUS LOAD CHANGE

Time (Sec.)	Load value P(W)+jQ(var)	Change status	position	DIC 1 detail coefficient			DIC 2 detail coefficient			DIC 3 detail coefficient		
				before	after	ratio	before	after	ratio	before	after	ratio
1	1000+j400	Add	Load2	1.5e-15	4.6e-5	3.1e+10	1.1e-14	1.6e-3	1.5e+11	8.0e-15	2.0e-4	2.6e+10
2	100+j50	Add	Load3	3.6e-12	2.1e-6	5.9e+5	7.0e-12	1.0e-5	1.4e+6	3.6e-12	3.5e-4	9.7e+7
3	500+j200	Add	Load1	4.0e-12	7.3e-4	1.8e+8	7.2e-12	1.8e-4	2.5e+7	4.4e-12	2.4e-5	5.5e+6
4	500+j200	removed	Load2	5.7e-12	4.3e-6	7.5e+5	1.1e-11	7.5e-5	6.8e+6	6.0e-12	1.8e-5	3.0e+6
5	1000+j400	Add	Load3	2.8e-11	5.9e-6	2.1e+5	1.8e-10	2.0e-4	1.1e+6	7.0e-11	1.6e-3	2.3e+7
6	200	Add	Load2	2.3e-11	2.1e-4	9.1e+6	1.9e-10	7.2e-3	3.8e+7	7.1e-11	9.2e-4	1.3e+7
7	500+j200	removed	Load3	3.9e-11	2.0e-6	5.1e+4	1.6e-10	2.0e-5	1.3e+5	5.6e-11	5.2e-4	9.3e+6
8	50+j500	Add	Load1	2.3e-11	2.6e-4	1.1e+7	2.4e-12	6.5e-5	2.7e+7	8.1e-10	8.3e-6	1.0e+4
9	100+j50	removed	Load3	2.4e-12	1.2e-7	5.0e+4	1.0e-10	4.0e-6	4.0e+4	3.8e-10	3.2e-5	8.4e+4
10	550+j700	removed	Load1	2.0e-11	2.1e-4	1.1e+7	8.1e-11	5.3e-5	6.5e+5	5.6e-10	6.8e-6	1.2e+4

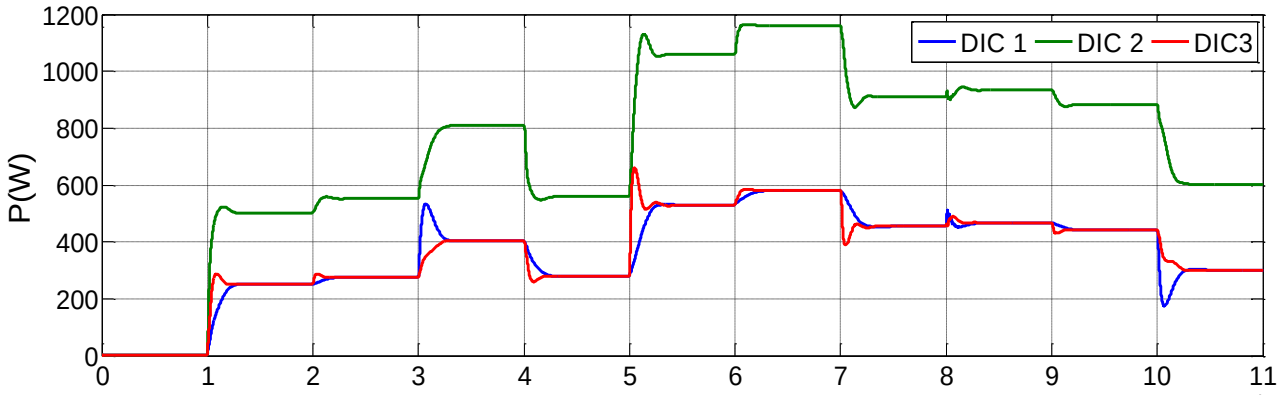

Fig. 13. Power of three DIC units with load change scenario as Table 2.

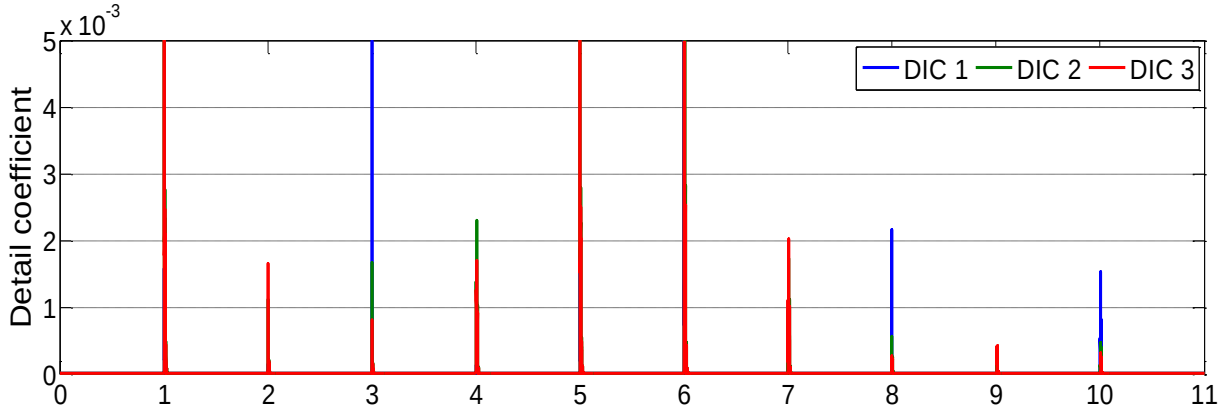

Fig. 14. Detail coefficient of three DIC units with load change scenario as Table 2.

Although the difference in coefficient before and after the load change or ratio of them depends on the load variation value and its position, but this difference or ratio is so large at any situation that the moment of load change is easily detectable in all DIC. The ratio of coefficient is not less than 10000 even in small load variation. This capability of the method makes it suitable for other application that needs synchronizing of the DIC unit in the microgrid.

6- CONCLUSION

This paper presents a new method for the frequency restoration in the islanded microgrid. This method does not require any communication link between DIC units. The detection of load change moment by the wavelet analysis is basic for synchronizing DIC unit. The simulation shows the proposed method is very efficient.

REFERENCES

[1] M. C. Chandrokar, D. M. Divan, and R. Adapa, “Control of parallel connected inverters in standalone ac supply systems,” IEEE Trans. Ind.Appl., vol. 29, no. 1, pp. 136–143, Jan./Feb. 1993.

[2] M. C. Chandrokar, D. M. Divan, and B. Banerjee, “Control of distributed ups systems,” in Proc. IEEE Power Electron. Spec. Conf., Jun., 1994,pp. 197–204.

[3] M. N. Marwali, J.-W. Jung, and A. Keyhani, “Control of distributed generation systems—Part II: Load sharing control,” IEEE Trans. PowerElectron., vol. 19, no. 6, pp. 1551–1561, Nov. 2004.

[4] K. D. Brabandere, B. Bolsens, J. V. denKeybus, A. Woyte, J.Driesen, andR. Belmans, “A voltage and frequency droop control method for parallel inverters,” IEEE Trans. Power Electron., vol. 22, no. 4, pp. 1107–1115,Jul. 2007.

[5] E. Barklund, N. Pogaku, M. Prodanovic, C. Hernandez-Aramburo, and T.C. Green, “Energy management in autonomous microgrid using stability constrained droop control of inverters,” IEEE Trans. Power Electron.,vol. 23, no. 5, pp. 2346–2352, Sep. 2008.

[6] D. De and V. Ramanarayanan, “Decentralized parallel operation of inverters sharing unbalanced and nonlinear loads,” IEEE Trans. Power Electron., vol. 25, no. 12, pp. 3015–3025, Dec. 2010.

[7] C. K. Sao and P. W. Lehn, “Autonomous load sharing of voltage source converters,” IEEE Trans. Power Del., vol. 20, no. 2, pp. 1009–1016, Apr.2005.

[8] J. M. Guerrero, L.G. deVicuna, J.Matas,M.Castilla, and J.Miret, “Output impedance design of parallel-connected UPS inverters with wireless load sharing control,” IEEE Trans. Ind. Electron., vol. 52, no. 4, pp. 1126–1135,Aug. 2005.

[9] Y. W. Li and C. N. Kao, “An accurate power control strategy for power electronics-interfaced distributed generation units operating in a low voltage multibus microgrid,” IEEE Trans. Power Electron., vol. 24, no. 12,pp. 2977–2988, Aug. 2009.

[10] J. He and Y. W. Li, "An enhanced microgrid load demand sharing strategy," IEEE Trans. Power Electron., vol. 27, no. 9, pp. 3984 - 3995, Sep. 2012.

[11] C. T. Lee, C. C. Chu, and P. T. Cheng, "A new droop control method for the autonomous operation of distributed energy resource interface converters," IEEE Trans. Power Electron., vol. 28, no. 4, pp. 1980 - 1993, Apr. 2013.

[12] J. M. Guerrero, J. C. Vasquez, J. Matas, L. G. de Vicuna, and M. Castilla, "Hierarchical control of droop-controlled AC and DC microgrids: A general approach toward standardization," IEEE Trans. Ind. Electron., vol. 58, no. 1, pp. 158–172, Jan. 2011.

[13] A. Bidram and A. Davoudi, "Hierarchical structure of microgrids control system," IEEE Trans. Smart Grid, 2012, vol. 3, no. 4, pp. 1963–1976, Dec. 2012.

[14] Y. A. R. I. Mohamed and A. A. Radwan, "Hierarchical control system for robust microgrid operation and seamless mode transfer in active distribution systems," IEEE Trans. Smart Grid, vol. 2, pp. 352–362, Jun. 2011.

[15] E. A. A. Coelho, P. C. Cortizo, and P. F. D. Garcia, “Small-signal stability for parallel-connected inverters in stand-alone ac supply systems,” IEEE Trans. Ind. Appl., vol. 38, no. 2, pp. 533–542, Mar./Apr. 2002.

[16] N. Pogaku, M. Prodanovic, and T. C. Green, “Modeling, analysis and testing of autonomous operation of an inverter-based microgrid,” IEEE Trans. Power Electron., vol. 22, no. 2, pp. 613–625, Mar. 2007.

[17] E. Barklund, N. Pogaku, M. Prodanovic, C. Hernandez-Aramburo, and T. C. Green, "Energy management in autonomous microgrid using stability-constrained droop control of inverters," IEEE Trans. Power Electron., vol. 23, no. 5, pp. 2346–2352, Sep. 2008.

[18] Y. A.-R. I. Mohamed and E. F. El-Saadany, "Adaptive decentralized droop controller to preserve power sharing stability of paralleled inverters in distributed generation microgrids,"

IEEE Trans. Power Electron., vol. 23, no. 6, pp. 2806–2816, Nov. 2008.

[19] S. V. Iyer, M. N. Belur, and M. C. Chandorkar, "A generalized computational method to determine stability of a multi-inverter microgrid," IEEE Trans. Power Electron., vol. 25, no. 9, pp. 2420–2432, Sep. 2010.

[20] S. G. Mallat, "A theory for multiresolution signal decomposition: The wavelet representation," IEEE Trans. Pattern Anal. Mach. Intell., vol.1, no. 7, pp. 674–693, Jul. 1989

.